AD-A019 186

# PASSIVE NOSETIP TECHNOLOGY (PANT) PROGRAM

M. R. Wool

Acurex Corporation

Prepared for:

Space and Missile Systems Organization

June 1975

SAMSO-TR-75-250

# FINAL SUMMARY REPORT PASSIVE NOSETIP TECHNOLOGY (PANT) PROGRAM

M. R. Wool
Aerotherm Division/Acurex Corporation
485 Clyde Avenue
Mountain View, California 94042

June 1975

AEROTHERM REPORT 75-159

Final Report for Period 1971 - 1975



Prepared for

SAMSO/RSSE
P.O. Box 92960
Worldway Postal Center
Los Angeles, California 90009

# REPORT DOCUMENTATION PAGE

READ INSTRUCTIONS BEFORE COMPLETING FORM

| | |
|---|---|
| 1. REPORT NUMBER: SAMSO-TR-75-250 | 2. GOVT ACCESSION NO. |
| 3. RECIPIENT'S CATALOG NUMBER | |
| 4. TITLE (and Subtitle): FINAL SUMMARY REPORT PASSIVE NOSETIP TECHNOLOGY (PANT) PROGRAM | 5. TYPE OF REPORT & PERIOD COVERED: Final Report; 1971 - 1975 |
| | 6. PERFORMING ORG. REPORT NUMBER: AEROTHERM REPORT 75-159 |
| 7. AUTHOR(s): M. R. Wool | 8. CONTRACT OR GRANT NUMBER(s): F04701-71-C-0027 CDRL A003 |
| 9. PERFORMING ORGANIZATION NAME AND ADDRESS: Aerotherm Division/Acurex Corporation 485 Clyde Avenue Mountain View, CA 94042 | 10. PROGRAM ELEMENT, PROJECT, TASK AREA & WORK UNIT NUMBERS |
| 11. CONTROLLING OFFICE NAME AND ADDRESS: SAMSO/RSSE P.O. Box 92960, Worldway Postal Center Los Angeles, CA 90009 | 12. REPORT DATE: June 1975 |
| | 13. NUMBER OF PAGES: 47 |
| 14. MONITORING AGENCY NAME & ADDRESS(if different from Controlling Office): N/A | 15. SECURITY CLASS. (of this report): Unclassified |
| | 15a. DECLASSIFICATION/DOWNGRADING SCHEDULE: N/A |

16. DISTRIBUTION STATEMENT (of this Report)

A

Approved for public release; Distribution Unlimited

17. DISTRIBUTION STATEMENT (of the abstract entered in Block 20, if different from Report)

18. SUPPLEMENTARY NOTES

N/A

**COLOR ILLUSTRATIONS REPRODUCED IN BLACK AND WHITE**

19. KEY WORDS (Continue on reverse side if necessary and identify by block number)

| | | | |
|---|---|---|---|
| Ablation | Heat transfer | Recession | Transition |
| Arc jet tests | Hydrometeors | Reentry physics | Thermochemistry |
| Boundary layers | Hypersonic flow | Roughwall effects | Weather effects |
| Graphite | Mass loss | Shape change | Wind tunnel testing |
| Inviscid flow | Nosetip technology | Shock layer | |

20. ABSTRACT (Continue on reverse side if necessary and identify by block number)

A summary of the analytical and experimental activities performed on the Passive Nosetip Technology (PANT) program is given. The various test programs are identified and key test results are described. Analysis results in the areas of surface roughness effects on nosetip performance, nosetip shape change physics, graphite ablation modeling, and weather erosion effects modeling are summarized. Program results indicate the direction for future development of reentry vehicle nosetip materials and configurations.

ACKNOWLEDGMENT

Aerotherm/Acurex wishes to acknowledge the significant contributions of Mr. W. E. Welsh and Dr. R. L. Baker of the Aerospace Corporation and Mr. Frank Baltakis of the Naval Surface Weapons Center to the technical success of this program. Furthermore, special thanks go to Mr. G. L. Denman of the Air Force Materials Laboratory for providing graphite ablation data from arc heater and ballistic range tests.

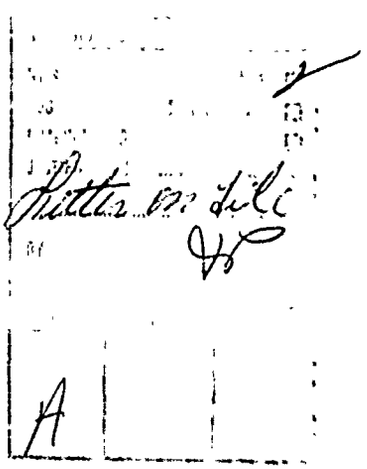

Preceding page blank

## FOREWORD

This document is the final summary report for the Passive Nosetip Technology (PANT) program. The program was administered by the Air Force Space and Missile Systems Organization (SAMSO/RSSE) under Contract F04701-71-C-0027 between 1 April 1971 and 30 June 1975 with the following project officers:

- Maj. L. Hildebrand
- Lt/Capt. A. L. Hunt
- Lt. A. T. Hopkins
- Lt. E. G. Taylor

During the program the following Aerospace Corporation personnel served as principal technical monitors on this program:

- W. E. Welsh
- C. Melfi
- W. Portenier

The work was performed by the Aerotherm Division of the Acurex Corporation, Mountain View, California. The following people were Aerotherm Project Managers during the program:

- Dr. R. M. Kendall
- R. A. Rindal
- D. L. Baker
- Dr. R. E. Lundberg

Wind tunnel testing was performed at Tunnel No. 8, Naval Surface Weapons Center, Silver Springs, Maryland with Mr. F. Baltakis serving as test engineer.

Numerous interim reports and technical memoranda were published during the program to document the analytical and experimental results of the program. A summary of interim report documents is as follows:

Volume I — Program Overview (U)

Volume II — Environment and Material Response Procedures for Nosetip Design (U)

Volume III — Surface Roughness Data

Part I - Experimental Data

Part II — Roughness Augmented Heating Data Correlation and Analysis (U)

Part III — Boundary Layer Transition Data Correlation and Analysis (U)

Volume IV — Heat Transfer and Pressure Distributions on Ablated Shapes

Part I -- Experimental Data

Part II — Data Correlation

Volume V — Definition of Shape Change Phenomenology from Low Temperature Ablator Experiments

Part I — Experimental Data, Series C (Preliminary Test Series)

Part II — Experimental Data, Series D (Final Test Series)

Part III — Shape Change Data Correlation and Analysis

Volume VI — Graphite Ablation Data Correlation and Analysis (U)

Volume VII — Computer User's Manual, Steady-State Analysis of Ablating Nosetips (SAANT) Program

Volume VIII — Computer User's Manual, Passive Graphite Ablating Nosetip (PAGAN) Program

Volume IX — Unsteady Flow on Ablated Nosetip Shapes - PANT Series G Test and Analysis Report

Volume X — Summary of Experimental and Analytical Results

Volume XI — Analysis and Review of the ABRES Combustion Test Facility for High Pressure Hyperthermal Reentry Nosetip Systems Tests

Volume XII — Nosetip Transition and Shape Change Tests in the AFFDL 50 MW RENT Arc - Data Report

Volume XIII — An Experimental Study to Evaluate Heat Transfer Rates to Scalloped Surfaces - Data Report

Volume XIV — An Experimental Study to Evaluate the Irregular Nosetip Shape Regime - Data Report

Volume XV — Roughness Induced Transition Experiments - Data Report

Volume XVI — Investigation of Erosion Mechanics on Reentry Materials (U)

Volume XVII — Computer User's Manual, Erosion Shape (EROS) Computer Program

Volume XVIII — Nosetip Analyses Using the EROS Computer Program

Volume XIX — Hydrometeor/Shock Layer Interaction Study

Volume XX — Investigation of Flow Phenomena Over Reentry Vehicle Nosetips

Volume XXI — Flight Implications of Low Temperature Ablation Shape Data

Volume XXII — Coupled Erosion/Ablation of Reentry Materials

Volume XXIII — Reentry Vehicle Nosetip Response Analyses

This report series and the summary final report were prepared by Aerotherm Division/ Acurex Corporation under Contract F04701-71-C-0027. Interim Report Volumes I through IX covered PANT activities from April 1971 through April 1973. Volumes X through XV represent contract efforts from May 1973 to December 1974. Volumes XVI through XVIII describe the background, development, and check out of the PANT EROsion Shape (EROS) computer code performed under supplementary agreements to the Minuteman Natural Hazards Assessment Program (Contract F04701-74-C-0069) between April 1974 and March 1975. Volumes XIX through XXIII document additional analyses performed between December 1974 and June 1975.

This technical report has been reviewed and is approved.

EG Taylor

E. G. Taylor, Lt., USAF
Project Officer
Aero and Materials Division
Directorate of Systems Engineering
Deputy for Reentry Systems

## ABSTRACT

A summary of the analytical and experimental activities performed on the Passive Nosetip Technology (PANT) program is given. The various test programs are identified and key test results are described. Analysis results in the areas of surface roughness effects on nosetip performance, nosetip shape change physics, graphite ablation modeling, and weather erosion effects modeling are summarized. Program results indicate the direction for future development of reentry vehicle nosetip materials and configurations.

TABLE OF CONTENTS

## LIST OF ILLUSTRATIONS

LIST OF TABLES

## LIST OF SYMBOLS

| | | |
|---|---|---|
| $B'$ | nondimensional ablation parameter = $\dot{m}/\rho_e u_e C_H$ | -- |
| $C_H$ | Stanton number | -- |
| h | altitude | km |
| k | peak-to-valley roughness | mil |
| $K_\ell$ | laminar rough wall heating multiplier | -- |
| $K_t$ | turbulent rough wall heating multiplier | -- |
| $\dot{m}$ | surface ablation mass flux | $lbm/ft^2sec$ |
| M | Mach number | -- |
| P | pressure | atm |
| $R_N$ | nose radius | in, ft |
| Re | free stream unit Reynolds number | $ft^{-1}$ |
| Re* | sonic point unit Reynolds number | $ft^{-1}$ |
| $Re^*_\theta$ | sonic point momentum thickness Reynolds number | -- |
| S | surface wetted distance from nosetip | in. |
| T | temperature | °R |
| u | gas velocity | ft/sec |
| WSI | weather severity index = $\int_0^\infty \rho_c h \, dh$ | $km^2gm/m^3$ |
| X | axial distance from nosetip stagnation line | in. |
| 50 MW | AFFDL 50 MW RENT arc plasma generator | -- |
| $\eta_\ell$ | laminar rough wall heating correlation parameter = $Re_{2,R_N} k/\theta$ | -- |
| $\eta_t$ | turbulent rough wall heating correlation parameter = $Re_k \sqrt{C_{H_S}} (T_e/T_w)^{1.3}$ | -- |
| $\theta$ | boundary layer momentum thickness | ft |

| | | |
|---|---|---|
| $\mu$ | viscosity | lbm/ft-sec |
| $\rho$ | density | $lbm/ft^3$ |
| $\rho_e u_e C_H$ | heat transfer coefficient | $lbm/ft^2sec$ |
| $\rho_c$ | cloud liquid water content as a function of altitude | $gm/m^3$ |
| $\psi$ | disturbance parameter modifier = $0.1\ B' + (1 + 0.25\ B')\rho_e/\rho_w$ | -- |

Subscripts

| | |
|---|---|
| e | boundary layer edge |
| k | based on peak-to-valley roughness |
| o | supply conditions |
| s | smooth wall |
| t | turbulent |
| t,2 | total behind normal shock |
| w | wall or surface |
| $\infty$ | free stream |
| 2 | behind normal shock |

Superscripts

| | |
|---|---|
| * | sonic conditions |
| $\infty$ | infinity |

# SECTION 1

# INTRODUCTION

Advanced, high-performance, reentry vehicles require nosetips which insulate against severe aerothermal heating and which maintain shape symmetry to avoid vehicle aerodynamic dispersion. The desirability of a passive nosetip which performs its function without the need for accessory controls or subsystems limits the selection of the primary nosetip material. Of all candidates, graphitic materials such as polycrystalline graphite and graphitized carbon/carbon composite materials provide the best resistance to aerothermal recession (ablation). The low recession benefits of graphitic materials are, however, compromised because they are relatively brittle. Brittleness increases nosetip mass loss in natural hydrometeor environments (erosion) and decreases allowable thermostructural loads. Passive nosetip design must consider the trade-off between the recession safety margin (erosion plus ablation burn through) and the thermostructural safety margin (catastrophic fracture). It is unfortunate that an increase in recession margin (longer nosetip) is generally accompanied by a decrease in structural margin. Indeed, the optimum characteristics of nosetip materials and configurations are difficult to determine for many ICBM performance regimes. The PAssive Nosetip Technology (PANT) program was, therefore, instituted to improve nosetip design analysis techniques so that the recession and thermal response of candidate nosetip design concepts could be adequately assessed.

To maximize design procedure improvements, the Aerotherm Division of Acurex Corporation has employed sophisticated analytical and experimental techniques in the disciplines of aerodynamics, fluid mechanics, and thermodynamics. The general approach was to plan and conduct ground test experiments which elucidate the relevant physical events occuring during reentry, to model the physical events in a form for use in high speed digital computers, and to validate the computer modeling through comparisons with flight nosetip response data. Although this approach requires a time consuming process of test and evaluation on ground test and subscale systems, the general utility of the results are invaluable to the nosetip and reentry vehicle designer. Indeed, PANT results are in general use throughout the reentry

community. Utilization of PANT data or modeling techniques by all major reentry vehicle design groups in the nation is a testimony that the program objectives have been satisfied.

In this summary final report, the key experimental and analytical results and conclusion are reviewed and the impact of results on the design of reentry vehicle nosetips is discussed. Based on the efforts made during this program, recommendations are presented to improve, further, the survival probability and accuracy of advanced reentry vehicle systems. Section 2 presents a summary of nosetip experiments performed during the program. Section 3 summarizes analytical modeling techniques developed on the program. Section 4 identifies the most significant program achievements and recommends techniques for further performance improvements.

## SECTION 2

## NOSETIP PHENOMENA EXPERIMENTS

Under the PANT program and Air Force Material Laboratory sponsorship, numerous test series were planned and conducted, including:

- Wind tunnel heat transfer and pressure model experiments (PANT)
- Wind tunnel shape change experiments (PANT)
- Hyperthermal ground tests of reentry materials (AFML/PANT)

Calorimeter and pressure model experiments provided the fundamental data on the relevant nosetip phenomena, shape change experiments produced the data base for validating computational procedures, and hyperthermal ablation tests indicated the response mechanisms of actual reentry nosetip materials. The test series under the three categories are summarized in Sections 2.1, 2.2 and 2.3.

### 2.1 WIND TUNNEL HEAT TRANSFER AND PRESSURE MODEL EXPERIMENTS (PANT)

During the PANT program, Tunnel No. 8 at the Naval Surface Weapons Center (NSWC)* was used extensively to measure the effects of nosetip size, shape, and surface character on important aerothermal performance parameters. Table 1 summarizes important features of the respective PANT heat transfer and pressure model experiments. A total of 56 models was fabricated and instrumented for over 200 data runs. At the Mach 5 tunnel condition, air supply properties were controlled to vary the flow characteristics over the respective test models. Thus, several data runs were performed for each model installation. The models and test conditions were specifically designed to satisfy the respective test objectives.

Series A, B, C and J calorimeter models were nominally 0.08 inch thick nickel shells with up to 75 backwall thermocouples to measure streamwise and circumferential temperature distributions. The Series A, B, and C calorimeters were produced by electroforming nickel over an aluminum mandrel. The process was substantially less costly than conventional model machining. Series J models were smaller and shorter; thus they were economically machined from wrought nickel. The Series H calorimeter model consisted of a sectioned aluminum

*Formerly Naval Ordnance Laboratory (NOL).

TABLE 1. HEAT TRANSFER AND PRESSURE TEST SUMMARY

| Test Series[a] | Number of Model | Model Shapes | Model Types | Test Points | Freestream Unit Reynolds Number $10^{-6}$ ft$^{-1}$ | Angle of Attack (deg) | Test Objective | Interim Report Documentation |
|---|---|---|---|---|---|---|---|---|
| A | 9 | Sphere/Cone; Blunt/Cone | Calorimeters | 46 | 0.5 – 20. | 0. | Roughness Effects on Transition and Heat Transfer | Vol. III, Part I |
| B | 6 | Ablated Shapes | 3 Calorimeters 3 Pressure Models | 37 | 5.0 – 20. | 0.-10. | Ablated Shape Pressure and Heat Transfer | Vol. IV, Part I |
| C | 1 | Sphere/Cone | Calorimeter | 16 | 1.6 – 24. | 0.-40. | Smooth Calorimeter Checkout; Angle of Attack Heat Transfer | Vol. V, Part I |
| E | 1 | Ablated Shape | Pressure Model | 19 | 2.5 – 20. | 0. | Observe Pulsating Flow | Vol. II |
| G | 33 | Ablated Shapes | Pressure Model with Tip Replacement | 47 | 2.5 – 20. | 0.-5. | Map Pulsating Flow Regime | Vol. IX |
| H | 1 | Scallop Replica | Calorimeter | 7 | 2.6 – 21. | 0. | Measure Scallop Surface Heat Transfer | Vol. XIII |
| J | 6 | Sphere/Cone; Blunt/Cone | Calorimeter | 40 | 0.4 – 7.4 | 0. | Shape and Size Effects on Roughness Transition and Heat Transfer | Vol. XV |

[a]All tests conducted in Naval Surface Weapon Center, Tunnel No. 8, at Mach 5.

replica of an actual wind tunnel ablation model. This model simulated heat transfer to a nosetip with an ablated surface character. Segments were nomianlly 1/4-inch thick rings with up to four backwall thermocouples in each ring. For all nickel and aluminum calorimeter runs, heat transfer data were derived from the time-varying, thermocouple, temperature measurements.

One of the important nosetip parameters considered in the PANT heat transfer tests was the surface roughness. Models for Series A were constructed with peak-to-valley roughness dimensions from 0.005 mils to 80 mils in order to span the roughness of all candidate reentry vehicle nosetip materials. Smaller surface roughnesses (0.6 to 3 mil) were obtained by blasting the nickel shells with steel grit. Larger roughnesses (3 to 80 mils) were achieved by brazing copper particles to the nickel. Figure 1 shows the smooth (0.005 mil), 1.5 mil grit-blasted and the 80 mil brazed particle models. Figure 2 compares a cross section photomicrograph of a grit-blasted surface to a photomicrograph of a typical polycrystalline graphite RV material and illustrates that the calorimeter models simulate well the surface roughness of a graphite material. Figure 3 presents measured heat transfer rates from three Series A tests and demonstrates the significant effect of the sandgrain surface roughness.

Two types of pressure models were fabricated and tested. For Series B tests, the external configurations were identical to the ablated shape calorimeter models, but internal design allowed for surface pressure measurements. For Series E and G tests, special ablated shape models were instrumented with high frequency pressure transducers to measure the magnitude and frequency of surface pressure fluctuations. Typical pressure data at zero and non-zero angle-of-attack from the Series B tests are shown in Figure 4.

## 2.2 WIND TUNNEL SHAPE CHANGE EXPERIMENTS (PANT)

Nosetip tests of specially selected low temperature ablator materials were also performed in Tunnel No. 8 of the Naval Surface Weapon Center. The objective of these tests was to identify the interacting effects of aerothermal parameters on the response of passive nosetips. The various nosetip shape-change experiments conducted in the NSWC wind tunnel under the PANT program are summarized in Table 2. In these test series, 76 models were exposed to a range of flow conditions. Photographic coverage provided the primary shape response data.

Two materials, camphor and paradichlorobenzene, were found to have ablative characteristics suitable for mass loss tests at Mach 5 wind tunnel conditions where turbulent boundary layer flow could be achieved. Nosetip models were machined from billets formed by vacuum compression molding of granular material stock. The process is qualitatively similar to


Figure 1. Typical wind tunnel calorimeter models used to measure effect of roughness on transition and heating.

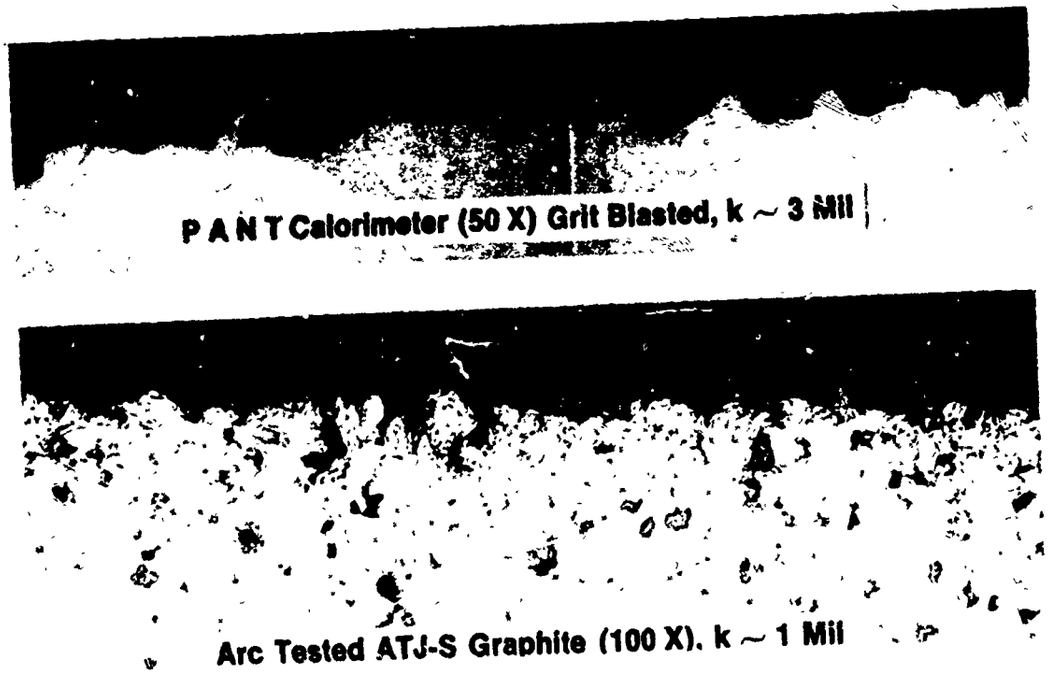


Figure 2. PANT calorimeter surface roughness compared to ablated graphite surface roughness.

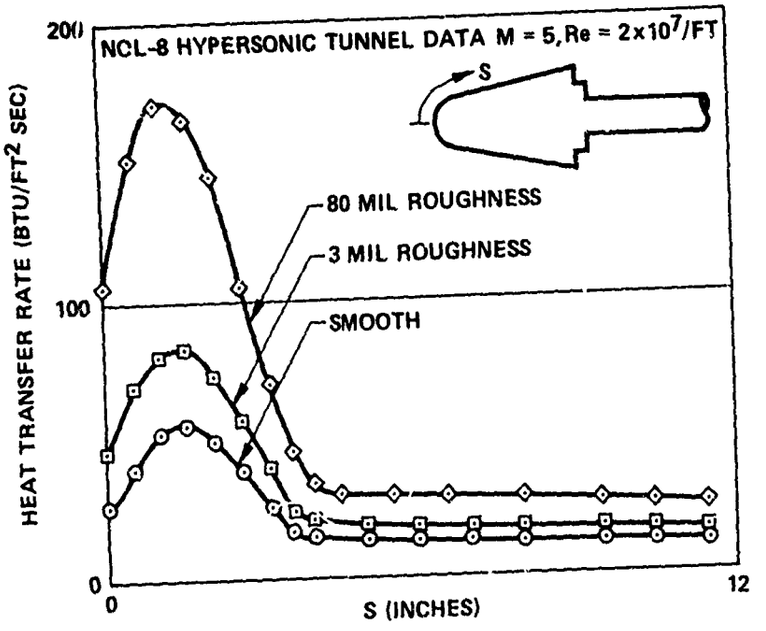


Figure 3. Rough surface heating data.

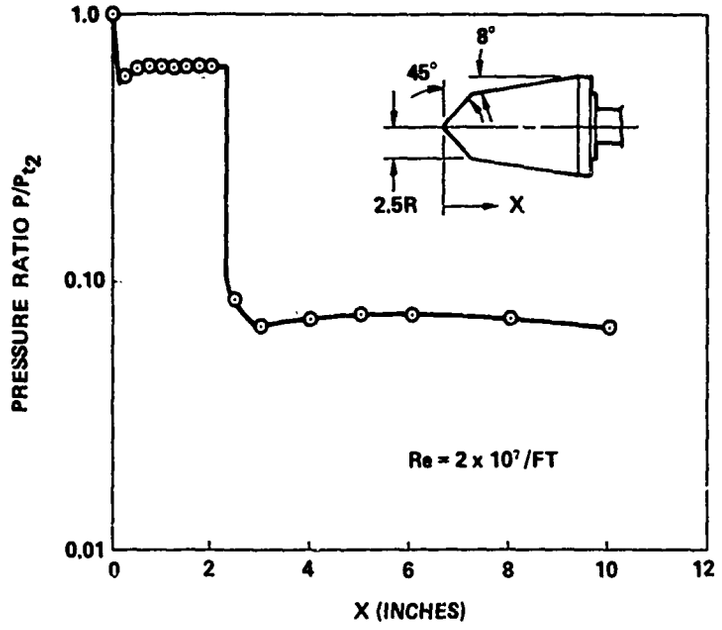


a. Zero angle-of-attack

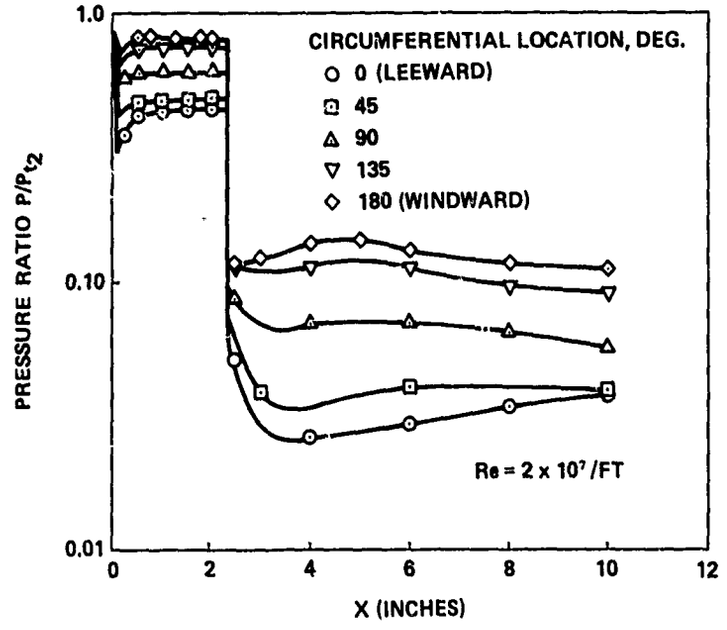


b. 10 degree angle-of-attack

Figure 4. Pressure data from Series B tests of 45/8 degree biconic configuration.

TABLE 2. WIND TUNNEL SHAPE CHANGE TEST SUMMARY

| Test Series | Number of Tests | Model Shapes | Material | Freestream Unit Reynolds Number $10^{-6}$ ft$^{-1}$ | Test Objectives | Interim Report Documentation |
|---|---|---|---|---|---|---|
| C | 23 | Sphere/Cone | PDB[a], Camphor, Combined | 1.7 – 9.7 | Compare Materials; Angle of Attack Shape Change | Vol. V, Part I |
| D | 18 | Sphere/Cone; Blunt Biconic | Camphor, Camphor with imbedded glass beads | 2.7 – 10.3 | Generate Shape Data to Validate Shape Change Computation Procedures | Vol. V, Part II |
| F | 4 | Sphere/Cone | Camphor | 4.0 – 9.0 | Variable Environment Shape Change | Status Report |
| I | 31 | Sphere/Cone; Laminar Profile; Blunt Biconics | Camphor, Camphor with imbedded glass beads | 0.8 - 15.7 | Quantify Effects of Reynolds Number, Roughness Initial Shape, Size, and Temperature on Irregular Shape Formation | Vol. XIV |

[a]paradichlorobenzene

polycrystalline graphite manufacture. The two materials were tested and compared in the Series C wind tunnel tests; and camphor was found to be best primarily because it provides the closest simulation to graphite flight response.

The low temperature ablator response data from Series C showed that the significant phenomena were well simulated in the wind tunnel tests. Figure 5 compares nosetip shape profile data from the wind tunnel with data from 50 MW arc heater ablation tests. Shape profiles at comparable flow combinations, such as sonic point momentum thickness Reynolds number, are quite similar. Series D, F, and I tests were performed to expand the number and range of environment and nosetip configuration variables. The variables include

- Initial Geometry — Sphere/Cone, Blunt/Cone, Various Biconics
- Model Size — 0.75 to 3.5 in shoulder radius
- Surface Roughness — Pure sintered camphor, 50 mil grooves, 1.3 to 7.5 mil glass beads
- Wall Temperature Ratio — $T_{wall}/T_{total}$ = 0.4, 0.8
- Sonic Point Unit Reynolds Number — $0.4 < Re^*/ft < 7 \times 10^6$ constant; also variable $Re^*$ runs

In the initial testing sequence it was observed that grossly irregular shapes formed at intermediate Reynolds number test conditions. These irregular shapes* are generally slender and exhibit significant tendency to be asymmetric even though the models are tested in uniform flow environments. The existence of such shapes in flight situations could significantly degrade reentry accuracy and may also lead to mission failure due to unsteady flow, increased ablation, or nosetip fractures. Thus, tests were optimized to study conditions leading to irregular shape formation. A summary of the pertinent camphor shape change data from all NSWC wind tunnel tests is given in Figure 6.

## 2.3 HYPERTHERMAL GROUND TESTS OF REENTRY MATERIALS (AFML/PANT)

During the PANT program, nosetip models of actual reentry materials were tested to identify ablation mechanisms and to provide data for validating analysis techniques. Tests included several materials, but Union Carbide ATJ-S graphite was emphasized. Table 3 summarizes the hyperthermal tests performed. AFML/PANT tests were sponsored by the Air Force Material Laboratory on concurrent programs but these tests provided the data to accomplish PANT

*Irregular shapes have also been termed "proboscidean" shapes.

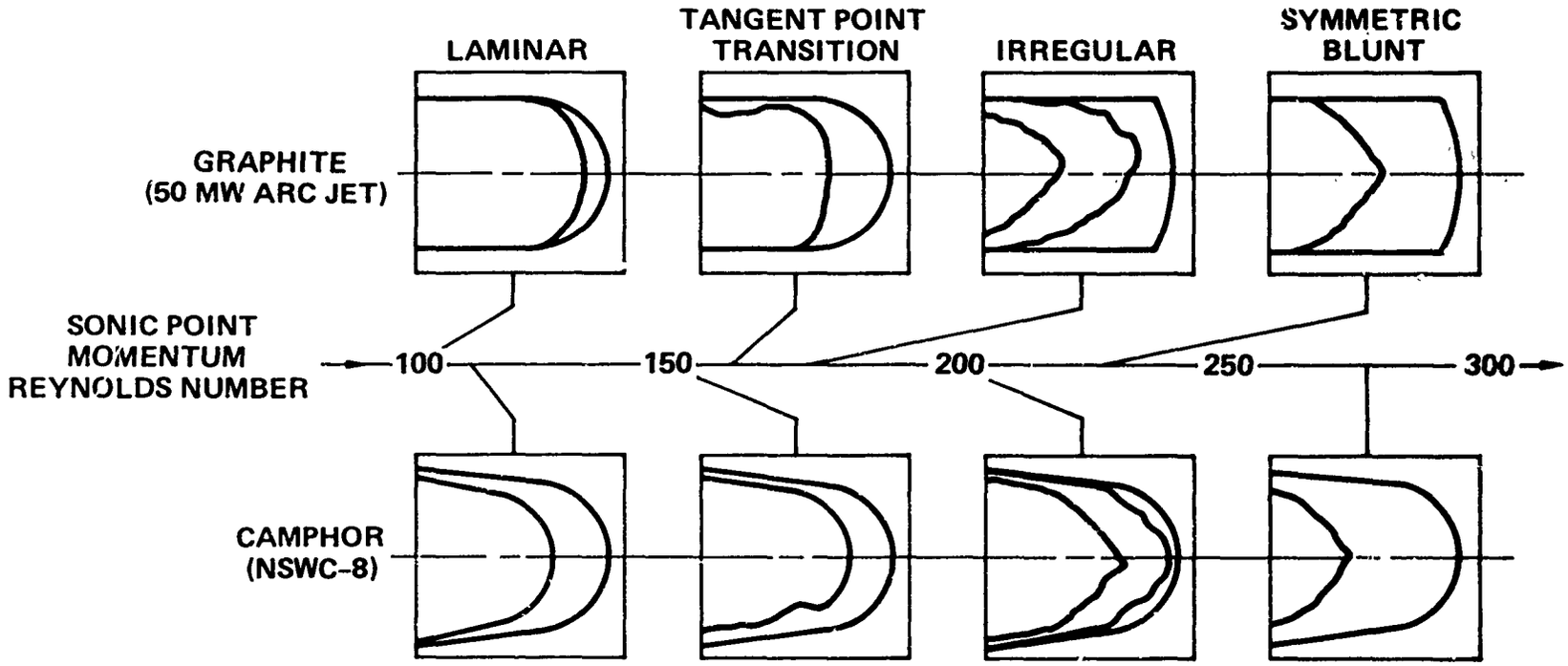


Figure 5. Nosetip shape dependence on flow regime including comparisons between graphite and low temperature ablator shape data.

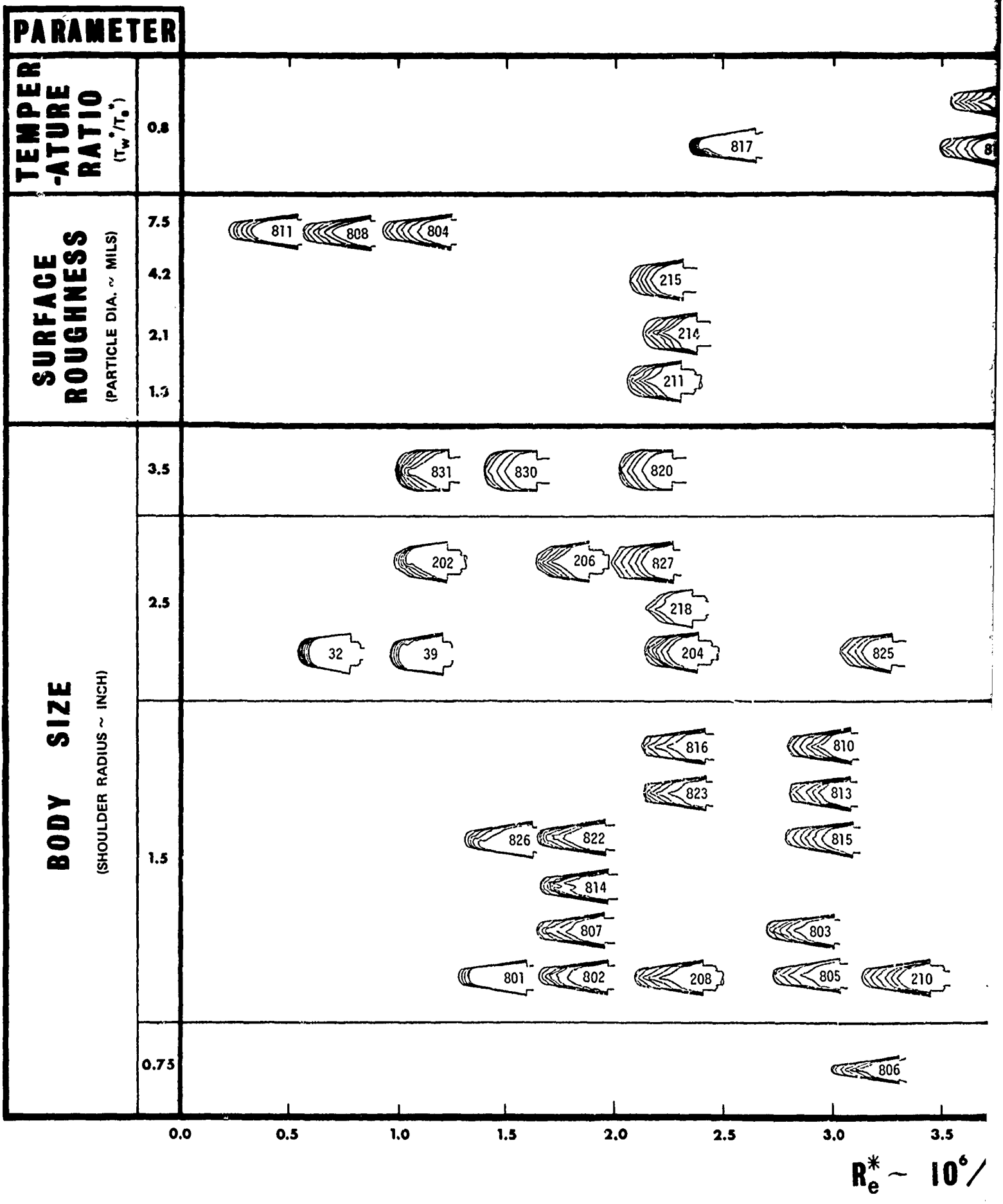


A

Figure 6. Summary of low temperature ablator (LTA) shap

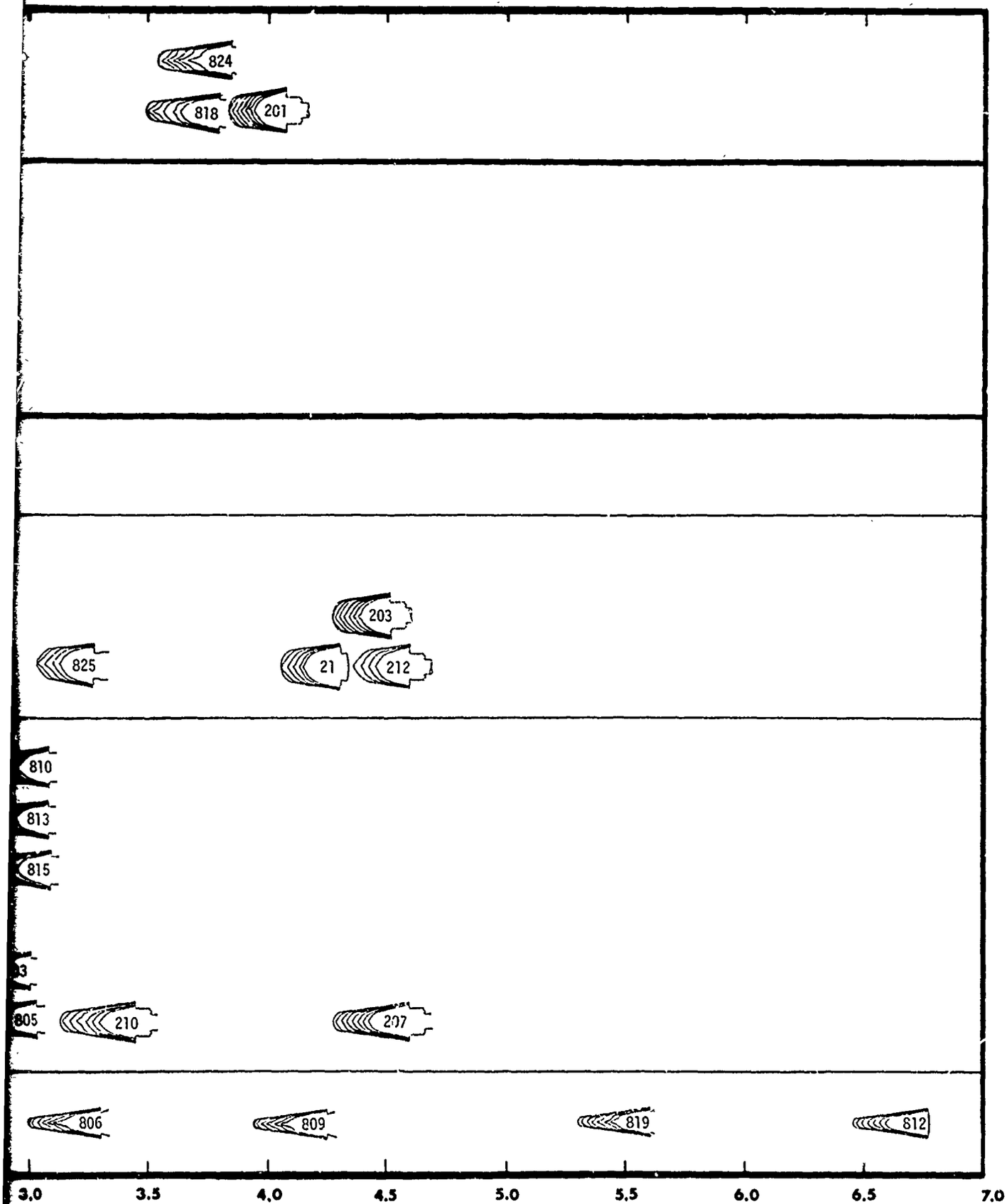


$R_e^* \sim 10^6/\text{ft.}$

Preceding page blank

blator (LTA) shape change data generated under the PANT program.



B

TABLE 3. HYPERTHERMAL ABLATION TEST SUMMARY

| Test Identification | Facility | Materials | Test Conditions | Test Objectives | Interim Report Documentation |
|---|---|---|---|---|---|
| ATM/PANT | AFFDL 50 MW RENT | 12 ATJ-S<br>7 3D-QP<br>6 MOD III-C/C | Stag Pressures: 20 atm to 100 atm<br>Peaked and Flat Enthalpy<br>Steady Conditions, M = 1.8 | Determine Ablation Mechanisms of Re-entry Materials | Vol. VI |
| AFVL/PANT | AEDC RANGE G | ~ 40 ATJ-S | Launch Velocities: 16 kfps to 18.5 kfps<br>Stag Pressures: 100 atm to 320 atm | Determine Ablation Mechanisms of ATJ-S Graphite | Vol. VI |
| PANT | AFFDL 50 MW RENT | 8 ATJ-S<br>5 ICCP<br>3 MOD III-C/C | Stag Pressures: 14 atm to 35 atm<br>Flat Enthalpy<br>Steady Conditions, M = 2.3, 3.0 | Study Shape Change and Transition of Reentry Materials | Vol. XII |

objectives. The data were generated in two facilities, the Flight Dynamics Laboratory (AFFDL) 50 MW RENT arc plasma generator and the Arnold Engineering Development Center (AEDC) Aeroballistic Range G.

The PANT AFML data, along with graphite sublimation data taken by Lundell at Ames Research Center, enabled a consistent, satisfactory explanation of the graphite ablation process. Simultaneous measurement of surface recession rate and surface temperature at known environmental test conditions provided the critical information. In the AFML/PANT ablation tests, the models in both the 50 MW arc and ballistic range tests were basically 1/2-inch diameter nosetips with various pretest shape profiles. The 50 MW arc tests were performed using peaked enthalpy flow conditions over a range of stagnation pressures. Ballistic range models were launched at nominally 18 kft/sec into range pressure conditions varying from 0.02 to 1.0 atm. Recession data were taken from photographic coverage and temperatures were measured pyrometrically in both facilities. Figures 7 and 8 show the ablation data from the respective test facilities plotted as a function of local pressure (either stagnation point or forecone sidewall).

The PANT tests in the AFFDL 50 MW arc were performed to observe boundary layer transition and shape change of reentry materials. Conditions were selected to study phenomena observed during the low-temperature-ablator wind tunnel tests. Specifically, the nozzle exit Mach number was maximized and pressure levels were reduced to produce marginally turbulent conditions where irregular (slender or asymmetric) shapes might occur. Although excellent shape change and transition data were obtained from the tests, arc enthalpies were lower than anticipated and conditions were more turbulent than desired. The measured shapes were consistent with turbulent shapes observed in the wind tunnel tests.

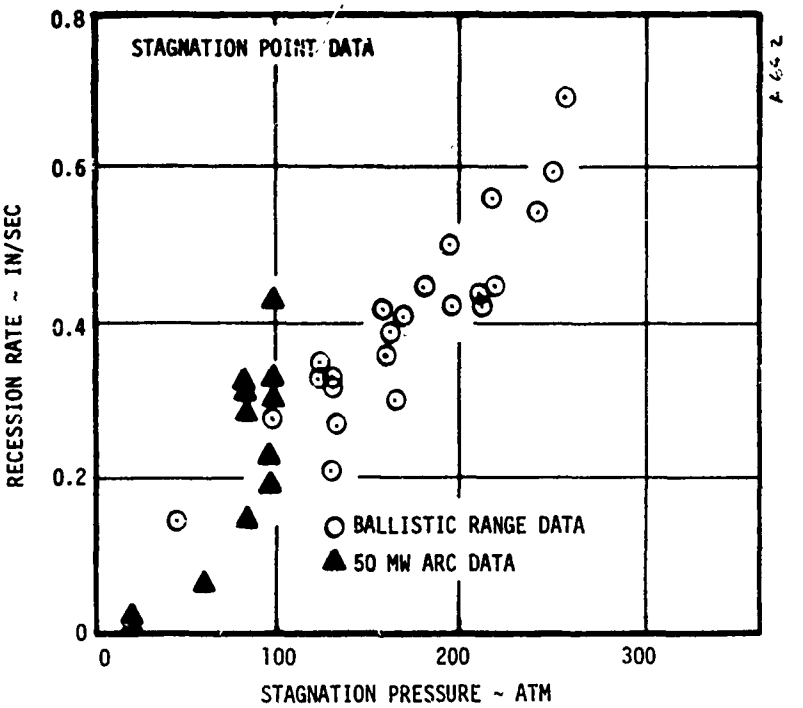


Figure 7. Summary of average stagnation point surface recession rates versus impact pressure for graphite models tested in the AFFDL 50 MW arc and the AEDC ballistic range G.

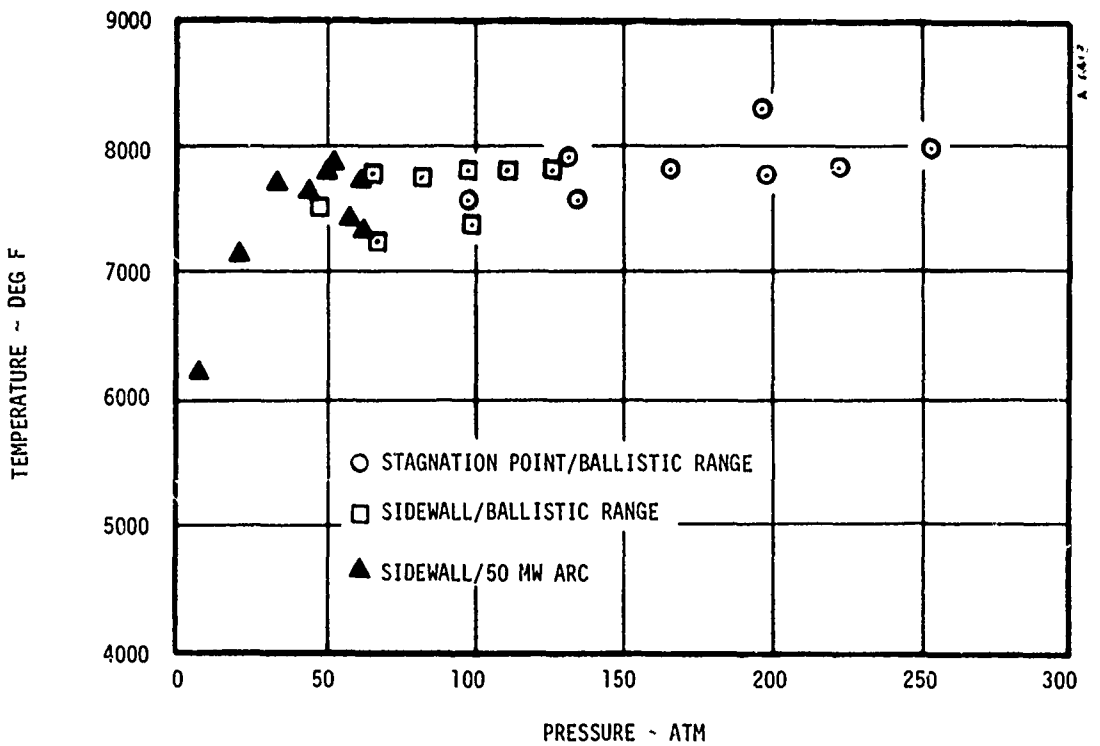


Figure 8. Summary of graphite surface temperature data from the AFFDL 50 MW arc and AEDC ballistic Range G test series.

## SECTION 3

## ANALYSIS OF NOSETIP PHENOMENA

Analysis efforts on the PANT program consisted primarily of data interpretation and correlation to develop procedures for the computerized evaluation of reentry vehicle nosetip response. The relevant physical phenomena are indicated schematically in Figure 9. Table 4 summarizes the various modeling improvements made to the genesis computer code which was developed on the Air Force Nosetip Design Analysis and Test Program (NDAT). Table 4 indicates the general breadth of efforts directed towards developing nosetip response technology. Table 5 summarizes supporting PANT reports by general technological area. Technical details of the significant PANT contributions are discussed in the following sections. These are:

- Surface Roughness Effects — Section 3.1
- Graphite Ablation Modeling — Section 3.2
- Shape Change Phenomenology — Section 3.3
- Coupled Erosion-Ablation Modeling — Section 3.4

### 3.1 SURFACE ROUGHNESS EFFECTS

Perhaps the most significant contribution of the PANT program is the fundamental recognition and quantification of material roughness effects on the performance of passive reentry vehicle nosetips. Based on wind tunnel calorimeter tests and subsequent data correlations, the effects of sandgrain roughness on boundary layer transition and heat transfer are well understood. The computational models which describe these phenomena are presented below.

#### 3.1.1 Roughwall Boundary Layer Transition

Two factors are needed to convert the laminar boundary layer on a nosetip to a condition of turbulence. There must be a source of disturbance, and there must be a means of amplifying the disturbance. If the disturbance is larger then less amplification potential is needed for transition and vice versa.

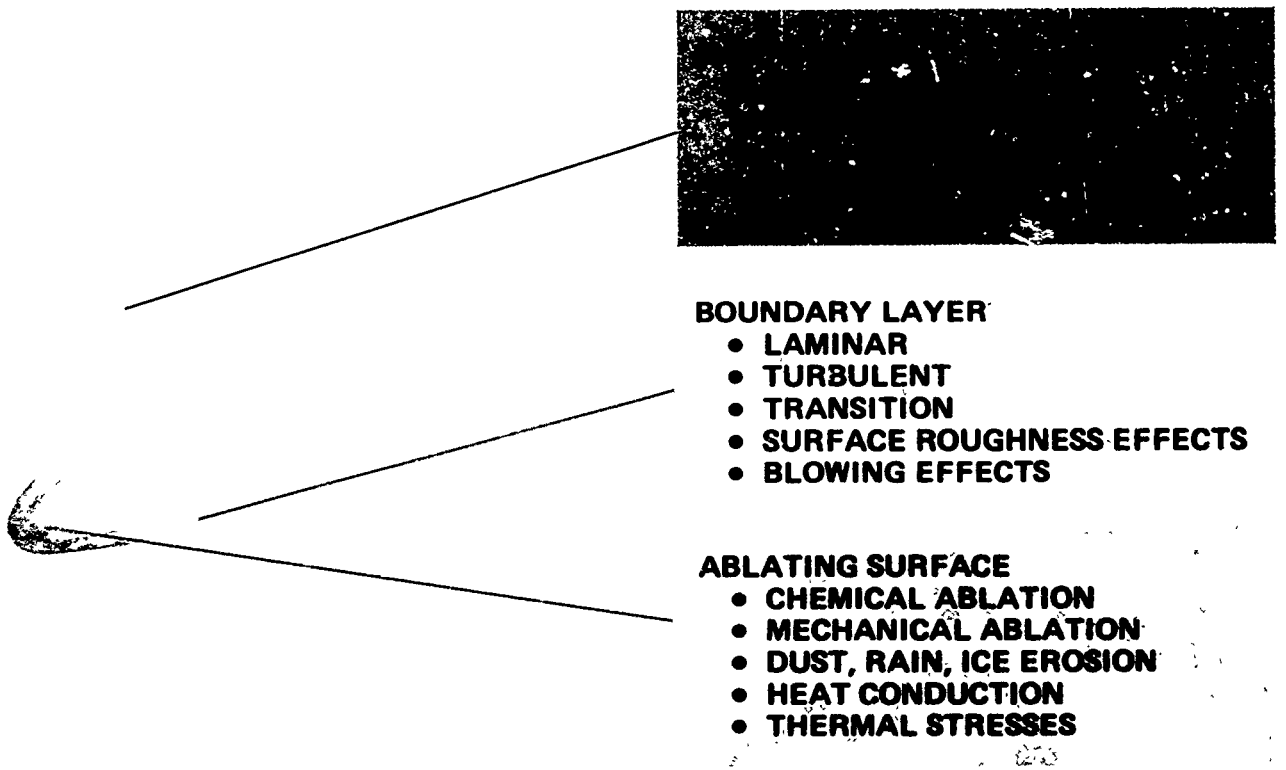


Figure 9. Modeling components of nosetip recession analysis.

## TABLE 4. SUMMARY OF MODELING IMPROVEMENTS

| Category | Phenomenon | Modeling Improvement | |
|---|---|---|---|
| | | NOAT Code | PANT |
| Shock Layer | Shock Shape | Based on sphere shock only | Supersonic shock expansion model |
| | Pressure Distribution | Tabular look up in blunt body solutions | Region correlations derived from exact flow calculations |
| | Flow Instabilities | Not considered | Criteria developed, but not included in computer code |
| | Particle Interactions | Not considered | Slowdown, ablation, and shattering modeled |
| Boundary Layer | Laminar Heating | | |
| | • Clear Air | Hoshizaki correlation | Improved property Fay-Riddell correlation implemented |
| | • Weather | Not considered | Incorporated erosion augmentation correlation |
| | Turbulent Heating | Momentum integral eqn | Incorporated unified skin friction formulation |
| | Transition | Smoothwall correlation with roughness modification | Unified correlation accounting for roughness, wall cooling, blowing and dissociation |
| | Surface Roughness | | |
| | • Transition | Correlation of sparse data, generally not used | Detailed fundamental correlation |
| | • Heating | Correlation of sparse data, generally not used | Detailed fundamental correlation, laminar and turbulent |
| | • Scallops | Not considered | Recognized importance, incorporated simple model |
| | Blowing Effects | | |
| | • Transition | Not considered | Included in unified correlation |
| | • Heat Transfer | Simple correlation used | Revised correlation |
| Ablating Surface | Chemical Ablation | Graphite only | Generalized surface chemistry employed (arbitrary material) |
| | Mechanical Ablation | Empirical correlation used | Shown to be negligible for graphite; melt modeled in chemistry package |
| | Erosion Mass Loss | Not considered | Material specific correlations coupled to surface ablation modeling |
| | Heat Conduction | Alternating direction explicit; steady state; heat of ablation methods | Coupled surface to 3-D heat conduction model; steady state options |
| | Thermal Stress | Tape coupling to elastic stress code | Off computer coupling to elastic-plastic stress code |
| Other | Shape Change Phenomenology | Biconic shapes not modeled | Identified shape regimes and shape change processes; implemented some modeling update; developed simplified recession analysis procedure |

TABLE 5. PANT REPORTS BY TECHNOLOGICAL AREA

| Technological Area | Interim Reports (Volume Numbers) |
|---|---|
| Transition Modeling | III, Parts I and III; X; XII; XV, XX, Theoretical Studies* |
| Heat Transfer | III, Parts I and II; IV, Parts I and II; XIII; XX |
| Erosion Modeling | XVI; XIX; XXII |
| Environment Modeling | IV, Parts I and II; IX; XX |
| Material Response Modeling Including Testing | VI; XI; XIII; Flight Transition Experiment*; Recession Sensor*; Shock Tube Feasibility; Erosion Facilities* |
| Shape Change Modeling | V, Parts I, II and III; XII; XIV; XXI |
| Flight Data Analysis | XVIII; XXI; XXIII |
| Nosetip Design | I; II; VII; VIII; X; XVII; Design and Material Constraints* |

*Status Report (Limited Distribution)

The sketch below shows the relationship between amplification potential and disturbance.

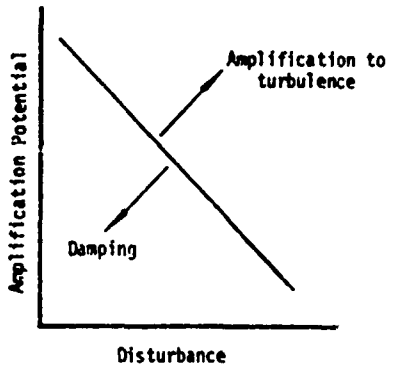


Amplification potential may be quantified by the momentum thickness Reynolds number based on conditions at the edge of the boundary layer. Disturbances may arise from several sources. The obvious ones include

- Turbulence in the freestream source flow
- Mass injection from or through the nosetip surface
- Vortices produced by surface roughness

For typical nosetip materials in reentry environments of interest, surface roughness is important primarily because boundary layer thickness is exceedingly small. A typical roughness of 0.0002 inch is a significant fraction of the boundary layer thickness.

Under the PANT program, transition location data from the NSWC wind tunnel tests allowed correlation of the turbulence amplification parameter in terms of a modified relative roughness disturbance parameter. Data demonstrated that the effective disturbance due to a roughness element is reduced as the surface to boundary layer edge temperature ratio increases. Analysis of the data showed that a higher surface temperature reduces the flow kinetic energy near the surface element. This result enabled extrapolation of the disturbance parameter to include the effects of ablation (mass injection) and dissociation on boundary layer transition. Figure 10 compares the transition onset correlation to the PANT wind tunnel data. The disturbance parameter has also been modified to include the effect of freestream turbulence, although the effect is important only for very smooth materials.

### 3.1.2 Roughwall Boundary Layer Heat Transfer

The effects of roughness on laminar and turbulent heat transfer are clearly indicated by the wind tunnel calorimeter data (see, for example, Figure 3). Semi-analytical correlation of these phenomena has enabled extrapolation to reentry conditions. The effect is modeled as

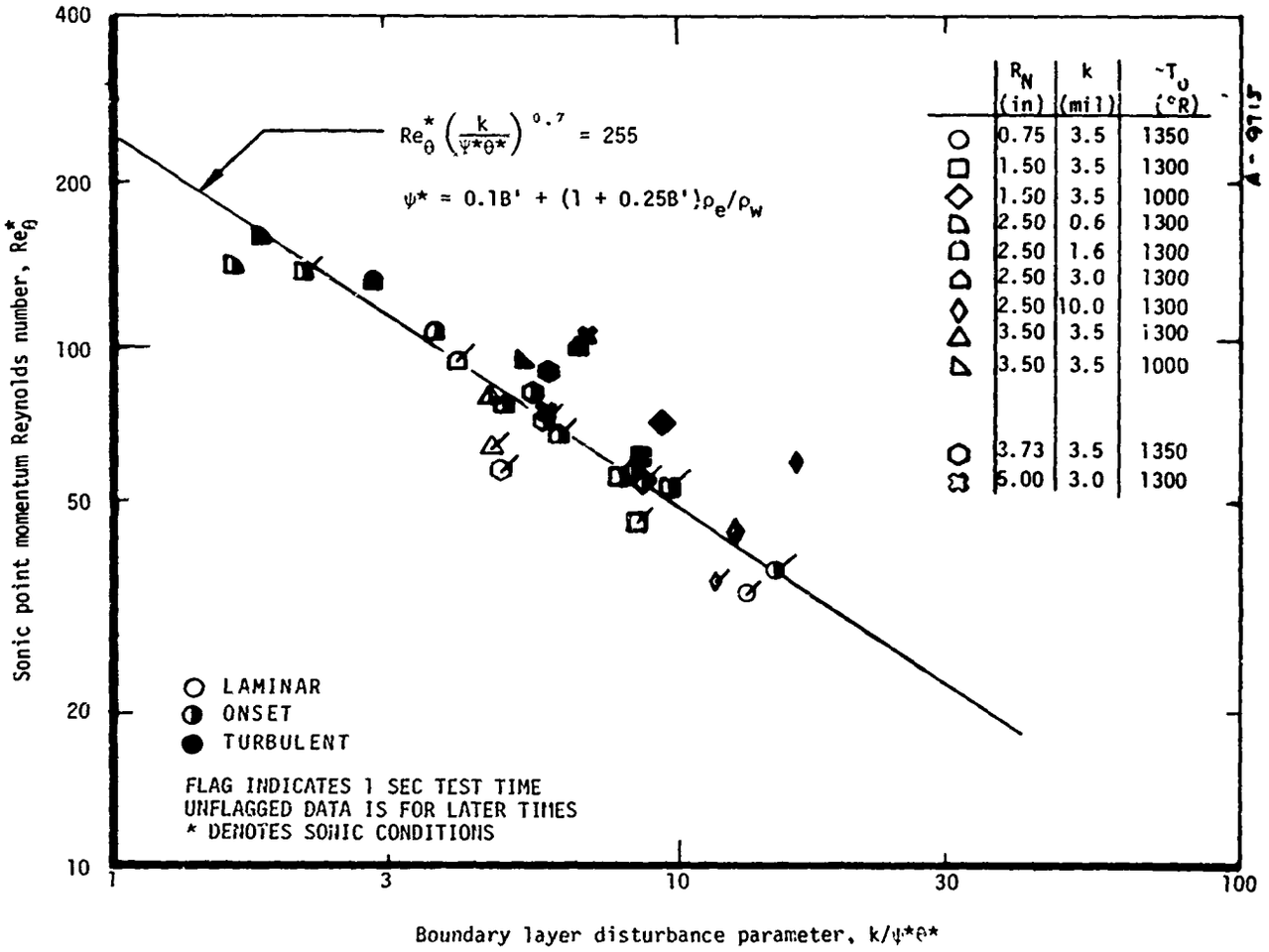


Figure 10. PANT transition onset criterion compared to wind tunnel data.

a multiplicative factor on the smooth wall boundary layer heat transfer. The roughwall skin friction is computed and used to evaluate the mass in the roughwall boundary layer. Thus, roughness affects both the edge conditions through the entropy swallowing and the heat transfer rate through the multiplicative factor.

The above comments apply equally to the laminar and turbulent computations. The laminar roughness heating factor correlation is shown compared to data in Figure 11. Figure 12 shows the effect of roughness on the turbulent boundary layer heat transfer. For typical conditions of interest, factors between 1.3 and 2.2 are experienced in turbulent flow. The form of the turbulent heating correlation was derived from the ratio of the roughness height to the laminar sublayer thickness. Approximations relate the sublayer thickness to suitable boundary layer edge and surface properties. Data profiles in Figure 12 cover a wide range of roughness heights, test conditions and nosetip locations. The agreement attests to the generality of the approach. Furthermore, under a concurrent AFML program, data from ballistic range calorimeters substantiated the correlation.

## 3.2 GRAPHITE ABLATION MODELING

The graphite ablation data obtained at hyperthermal, high pressure test conditions under concurrent AFML programs indicated the proper techniques for modeling graphite ablation phenomena. Three aspects of graphite mass loss modeling must be understood to achieve accurate predictions at reentry conditions. These are

- Surface thermochemical reactions between air and high temperature graphite
- Microparticle mass loss due to surface shear forces and/or preferential ablation (clear air)
- Ablation roughness producing increases in heat and mass transfer (scallops)

Surface temperature and ablation rate data taken over a wide range of conditions enable identification of appropriate modeling techniques. Table 6 indicates contributions of the PANT/AFML studies to graphite ablation technology. The primary result of the PANT/AFML studies was to show that roughness effects on heat and mass transfer explained major data prediction differences. Figure 13 compares predicted and measured recession rates for a range of aerodynamic conditions. Scatter is within the uncertainty in measuring shape and local recession rate.

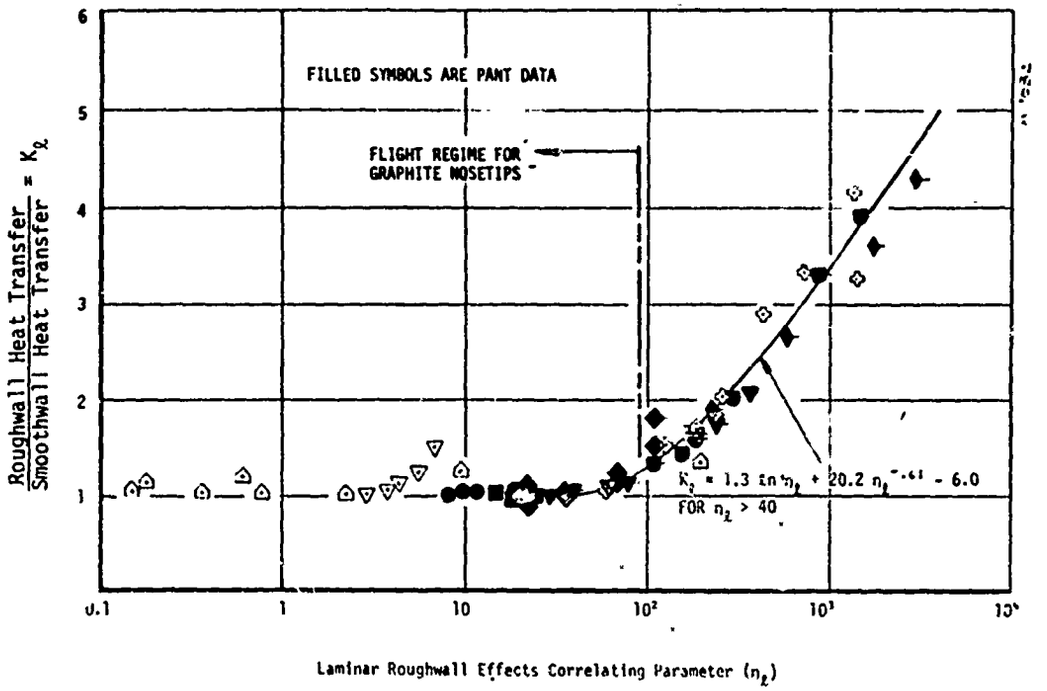


Figure 11. Roughwall effect on laminar heat transfer; PANT series A and other data.

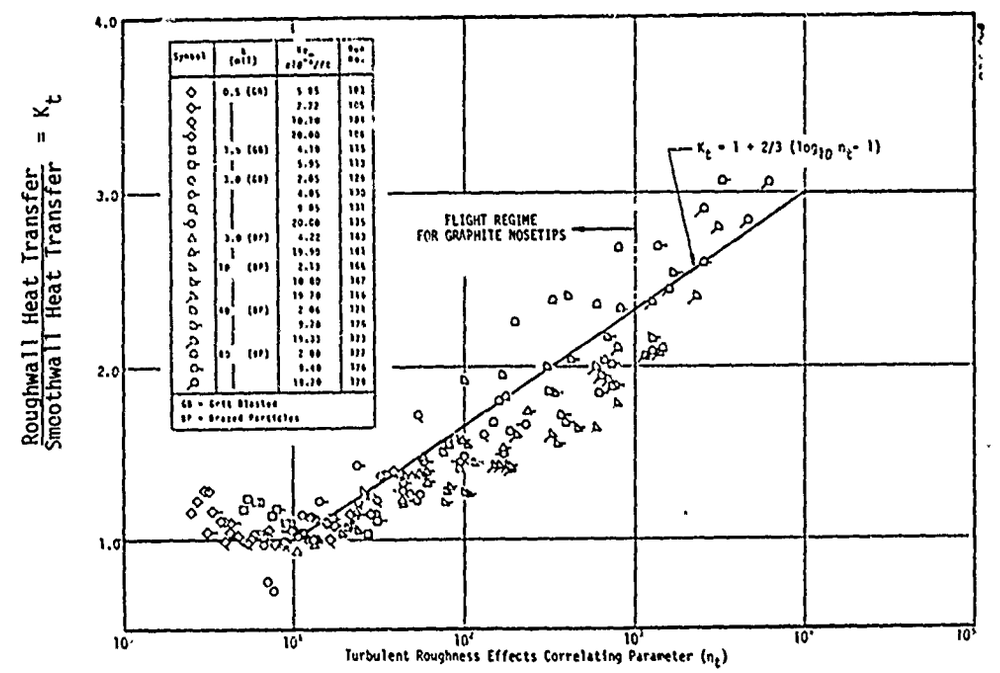


Figure 12. Roughwall effect on turbulent heat transfer.

TABLE 6. PANT/AFML CONTRIBUTIONS TO GRAPHITE ABLATION TECHNOLOGY

| Phenomenon | Details | Prior to PANT | PANT Model |
|---|---|---|---|
| Surface Thermochemistry | • Reaction Products: Sublimed Carbon, Oxides of Carbon, Nitrides of Carbon. | • Importance of Sublimation Kinetics Uncertain;<br>• $C_2N$ Species Not Considered | • Use JANNAF data and Equilibrium Chemistry, Including $C_2N$ Species |
| Micro Particle Mass Loss | • Considered as Additive or Multiplicative Increase to Chemical Ablation | • Factors up to 3 Used to Explain Flight Data | • Not Significant for High Quality Graphite Materials |
| Roughness Effects on Heat and Mass Transfer | • Multiplicative Effect on Smooth Surface Predictions | • Effect Uncertain, Often Ignored | • Very Important, Use PANT Correlation with Roughness = 2 to 5 mils |

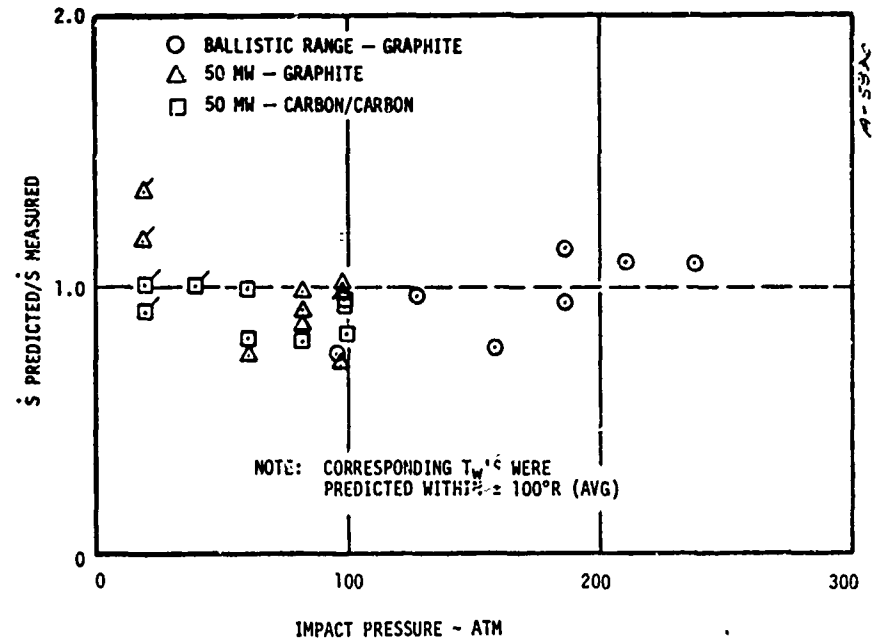


Figure 13. Summary of recession predictions compared with 50 MW and ballistic range data.

## 3.3 SHAPE CHANGE PHENOMENOLOGY

The low temperature ablator tests which were conducted under the PANT program provided valuable indications of nosetip response sensitivity to the quantities of interest to the nosetip designer. Reasonably complete experimental parameterization of aerodynamic conditions, initial nosetip shape, and material roughness provided a mapping of nosetip shape categories and pointed out the existence and cause of undesirable, ablation-induced, irregular nosetip shapes. Figure 14 shows the various shape profile categories that were observed.

Shape categories are determined by the occurrence of boundary layer transition and the formation of strong secondary shock flows. For post-sonic point transition (Category 2), asymmetric gouging in the vicinity of the cone tangent point can occur. The significance of this phenomenon in flight environments is not clear because increasing Reynolds number during reentry should quickly drive transition forward of the sonic point. Presonic point transition rapidly gouges the blunted nosetip. Depending on the symmetry of these transition gouges, the various secondary shock situations can occur (Categories 3, 4, and 5).

Critical to the formation of symmetric and asymmetric cusped shapes (Categories 3 and or 4) is the formation in the flow of a strong secondary bow shock. A strong secondary shock cannot form in the low Mach flow of an arc jet; thus, no similar shapes develop in ablation tests of reentry materials. Since flight Mach numbers are high, however, the shapes observed

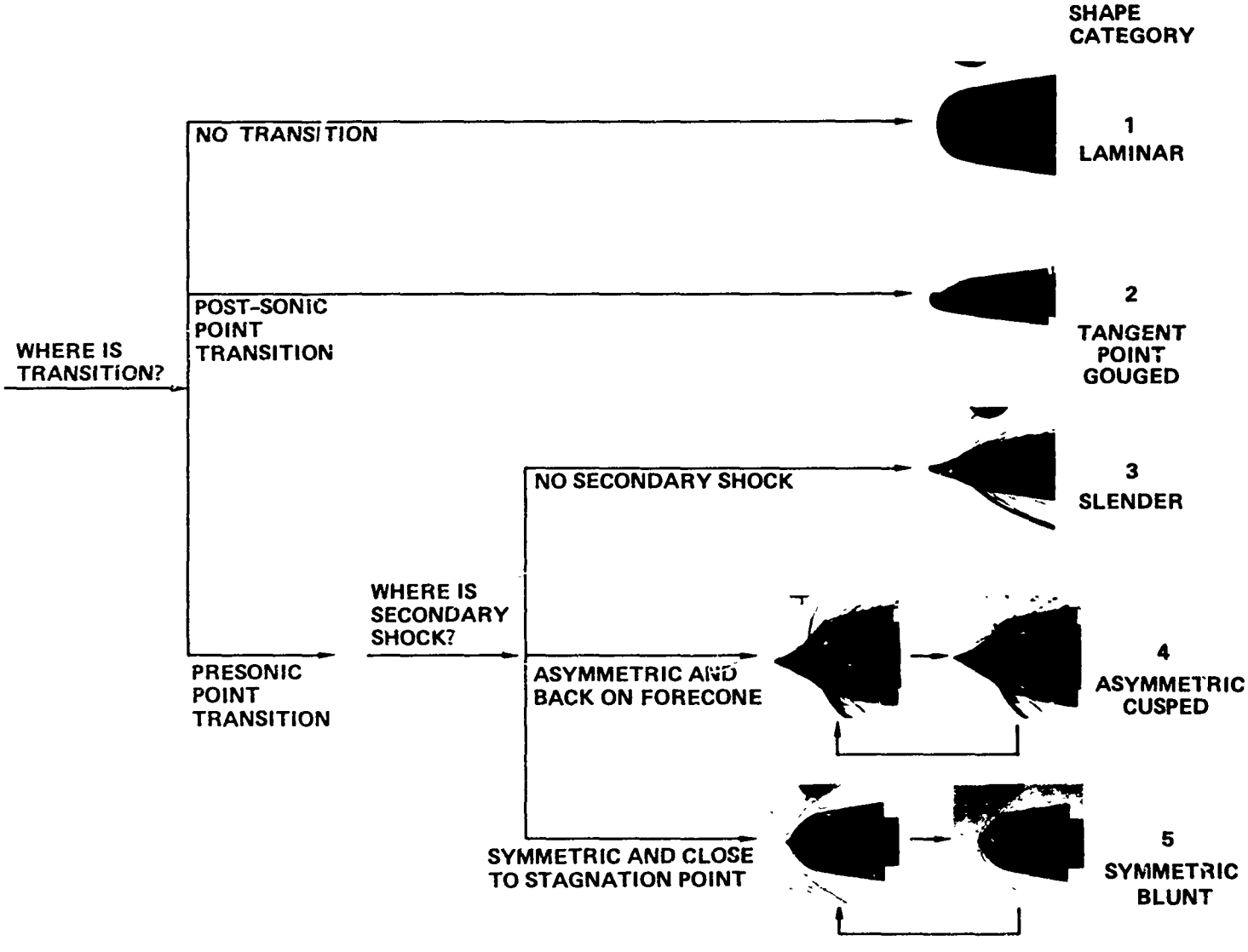


Figure 14. Nosetip shape categories determined from constant condition low temperature ablator tests.

in the wind tunnel tests are quite probable in flight situations. The chronology of a flight nosetip shape response may be described as follows:

- During the early portion of a trajectory (altitudes between 150 and 50 kft), the nosetip experiences laminar heating and ablation and approaches an ellipsoid-like shape.
- Transition occurs on the blunt shape between an altitude of 50 kft and 10 kft depending primarily on the roughness of the nosetip material; turbulent flow produces high recession off the nosetip centerline and the blunted nosetip is gouged.
- As transition gouges grow, the laminar blunt shape is reduced to a laminar cap followed by an ablation roughened sonic surface. The symmetry or asymmetry of the initial transition and the flow environment over the laminar cap control the shape category which develops (see Figure 14). For a typical trajectory, the final turbulent shape category becomes established approximately 10 kft to 20 kft below the transition onset altitude
- If the turbulent gouging of the laminar profile is completed before impact, then during the remainder of the flight, rapid recession of the established turbulent profile occurs

Based primarily on wind tunnel data, design criteria have been determined to identify under what conditions the formation of slender, asymmetric or cusped shapes is likely. The criteria are applied at the approximate altitude where transition gouging (sharpening) is complete. Two conditions must exist to avoid irregular cusped shapes:

$Re^*\theta(k/\psi\theta)^{0.7} \geq 425$ at sonic point of initial shape evaluated at the sharpened altitude

$Re^*R_N \geq 0.26 \times 10^6$ at sonic point of initial shape evaluated at the sharpened altitude

where

$Re^*$ = sonic point unit Reynolds number

$R_N$ = initial nose radius

$k$ = material roughness

$\psi$ = boundary layer disturbance modifier = $0.1\ B' + (1 + 0.25\ B')\rho_e/\rho_w$

$\theta$ = sonic point laminar momentum thickness

The first criterion insures that the terminal laminar cap is small, and the second criterion insures that the secondary shock effects occur close to the nosetip centerline. Application of these irregular shape criteria to flight conditions is discussed in Section 4.

## 3.4 COUPLED EROSION/ABLATION PHENOMENA

Data obtained on other Air Force programs have demonstrated that significant nosetip material can be removed during encounters with natural weather such as rain, snow, and ice particles. Analyses of hydrometeor effects on the nosetip response were performed on the PANT program and incorporated into the PANT computerized design analysis procedures. Weather influences the nosetip response because, relative to the high speed vehicle, the hydrometeor particles rapidly traverse the bow shock, impact the surface, and erode away some amount of mass. In addition, the associated disruptions to the flow over the model alter the nosetip response. Specifically, weather encounters affect nosetip response modeling as follows:

- Nosetip material is removed from the surface in the solid phase, thus increasing recession (this is generally termed "erosion")
- Hydrometeors and ejected nosetip material disrupt the bow shock and boundary layer flow so that heat and (probably) mass transfer are increased
- Surface craters increase the surface roughness and hence affect transition and roughwall heating phenomena
- Therefore, recession rate distributions are altered and shape profiles become different and generally blunter than in clear air

For brittle graphitic materials, erosion mass loss and associated increases in heat transfer are significant and could lead to failure of a nosetip or heat shield designed for clear air reentry.

Figure 15 shows the effect of increasing weather severity on the recession of a typical carbon/carbon composite nosetip. The dashed line represents the effect of weather if the effects of erosion on heat and mass transfer were ignored. Clearly this coupling has a significant effect on the nosetip response. Unfortunately, the effects of weather are not well characterized at the present time. Qualitatively, modeling uncertainties include:

- A factor of 2 to 10 uncertainty in the characterization of the weather environment (particle size, type, and concentration)
- A somewhat unknown effect of the bow shock layer on the hydrometeor particle

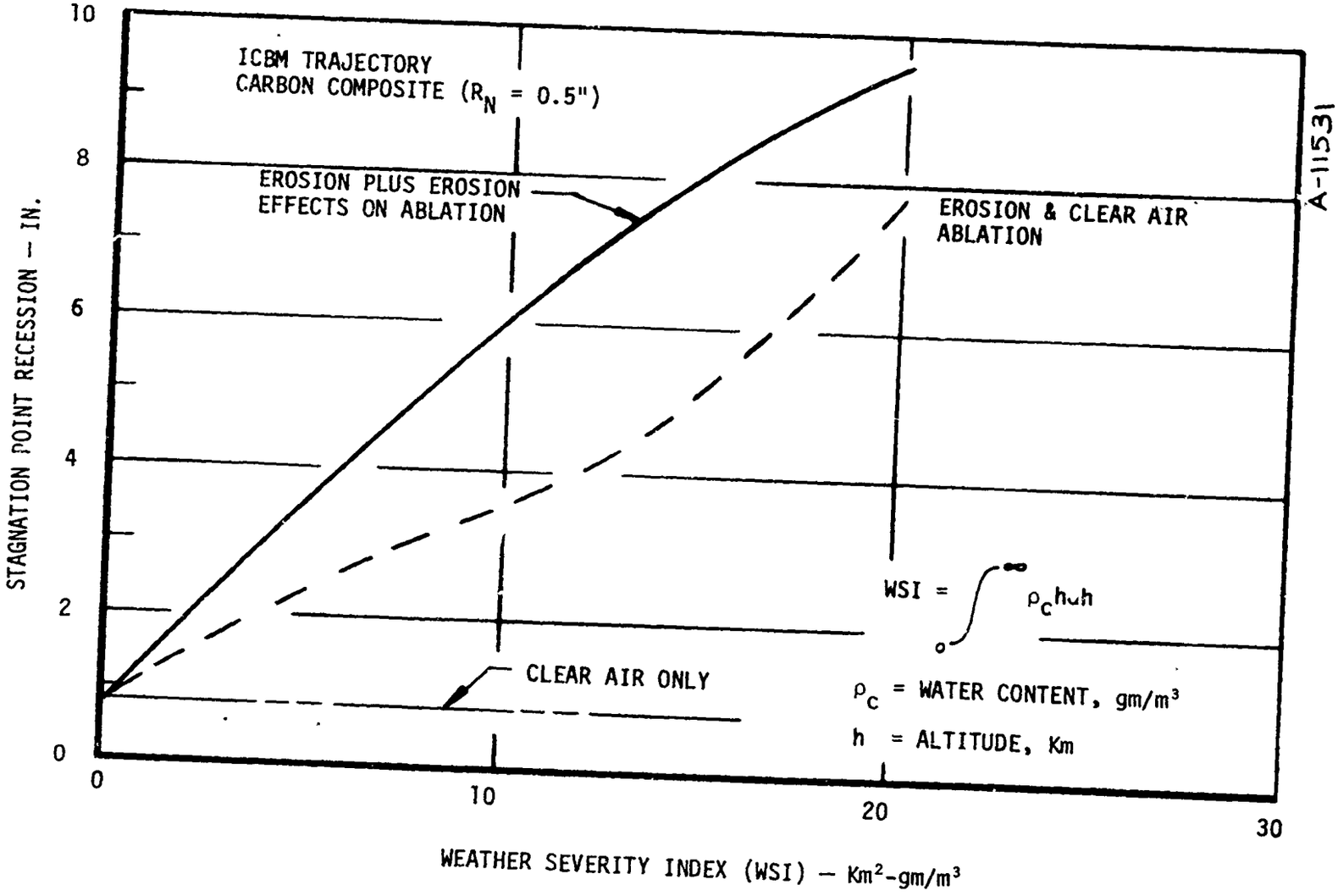


Figure 15. Effect of weather encounter on carbon composite nosetip recession.

- A factor of 2 to 5 uncertainty in the erosion mass loss in any particle impact
- A factor of 2 uncertainty in the coupled effects of erosion on transition and heat transfer

Thus, calculations of the type shown in Figure 15 must be used with a significant margin of safety in nosetip design analysis.

## SECTION 4

## CONTRIBUTIONS OF THE PASSIVE NOSETIP TECHNOLOGY PROGRAM

The three primary contributions of the Passive Nosetip Technology program to the improved understanding of flight vehicle nosetip performance are:

- The identification and quantification that the roughness of the nosetip material directly controls nosetip response
- The categorization of nosetip shapes which occur as a result of the aerothermal events during hypervelocity reentry
- The development of improved nosetip response analysis tools

The implications of these contributions to the design of reentry vehicle nosetips and nosetip materials are significant. Section 4.1 summarizes these implications, and Section 4.2 indicates how the contributions of the program can be utilized to develop nosetip configurations and material designs which will improve reentry vehicle accuracy and survival.

### 4.1 FLIGHT IMPLICATIONS

The quantitative characterization of the nosetip boundary layer transition event guides many aspects of reentry vehicle nosetip design because transition dramatically increases nosetip recession. Since transition depends on roughness, and recession and nosetip shape are critically related to transition, the roughness of nosetip materials is a significant design parameter. This important consideration is illustrated by the computer code calculations shown in Figures 16 and 17. Figure 16 presents the transition onset altitude as a function of nosetip surface roughness, and Figure 17 relates the resulting nosetip recession to roughness for two typical flight trajectories. These calculations are described fully in the Interim Report, Volume XVIII. The dramatic reduction in overall recession with reduced roughness is the reason nosetip designers and material fabricators have directed considerable effort towards development of smooth graphitic and carbon/carbon materials.

Utilization of smooth materials (roughness less than 0.3 mils) may, however, lead to undesirable nosetip shapes such as those seen in low-temperature-ablator shape change experiments

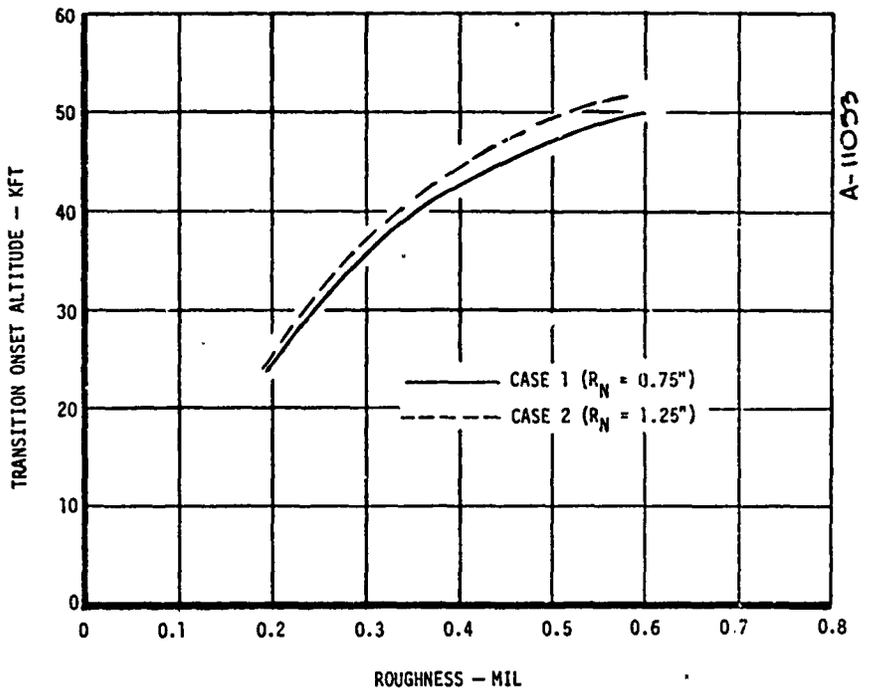


Figure 16. Sensitivity of transition altitude to material roughness.

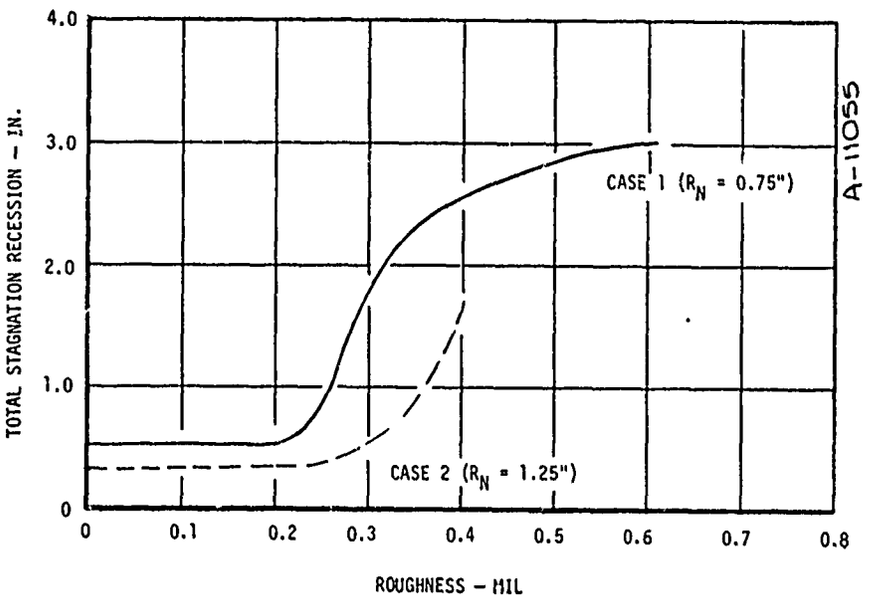


Figure 17. Sensitivity of recession to material roughness.

(Categories 2, 3, and 4 of Figure 14). Criteria derived from low-temperature-ablator shape change data provide an indication of the shapes which may develop during reentry as a function of material roughness. Figure 18 is an example which has been obtained for the 1.25 inch nose radius case shown in Figures 16 and 17. The figure indicates the altitude bands where various shape change categories are predicted as a function of the material roughness. For the particular configuration, material type, and trajectory combination analyzed, a cusped asymmetric shape (Category 4) is predicted for late in the trajectory if roughness is between 0.2 and 0.3 mils. Asymmetric shape change in the tangent point transition altitude band is generally small because cone recession is minimal. For larger roughness materials (greater than 0.3 mils), the probability of shape asymmetries is reduced, but the overall recession, as seen in Figure 17, is increased. This problem is compounded as nose radius is decreased because the altitude band required for nosetip sharpening is reduced.

A smoother material is also affected significantly by a weather encounter. Since weather, in the form of cirrus ice clouds, may occur at altitudes of 50,000 feet, the advantage of the smooth material, namely transition delay, will be negated by surface crater formation during the weather encounter. On the other hand, if a nosetip is designed for roughwall transition at 50,000 feet, then a cloud encounter will not dramatically alter boundary layer transition.

In general, the development of roughwall effects technology has indicated that careful selection of material roughness characteristics is a critical part of the overall nosetip system design. An overly rough material may lead to transition too high and to excessive recession; an overly smooth material may produce weather sensitivity and/or uncertain aerodynamic characteristics. The characteristics of an optimum nosetip material are indicated in the next section.

## 4.2 NOSETIP DESIGN GUIDELINES

No generally applicable nosetip design guideline can as yet be formulated because of the uncertainties in material characteristics and in the criteria defining nosetip shape performance. As materials and flight requirements evolve, nosetip system design will continue to require coordinated test and evaluation activities. Prototype materials and configurations must be ground tested to enable careful interpretation of ablation and erosion phenomena. Subscale flights should be performed and thoroughly analyzed to provide information on actual flight performance.

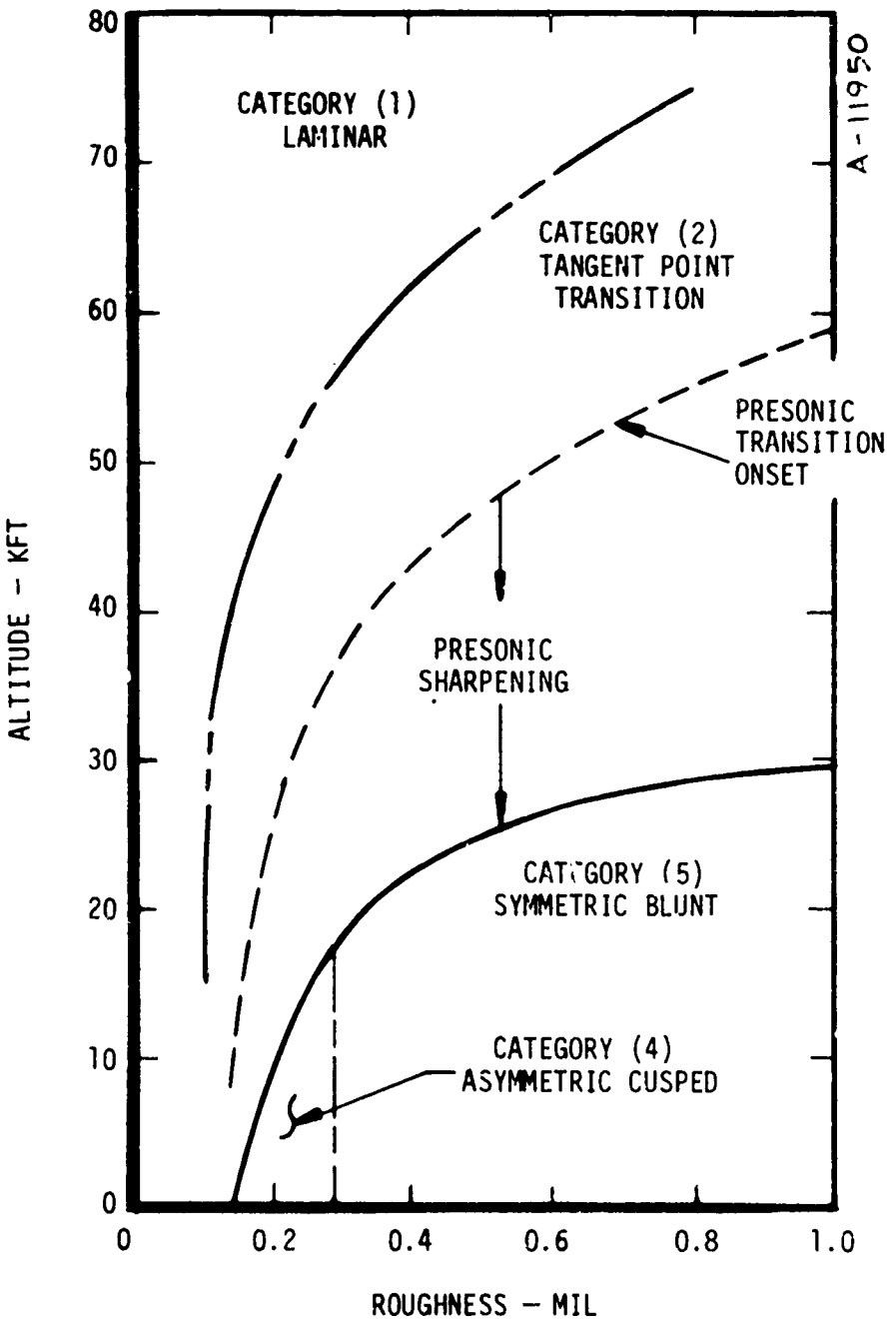


Figure 18. Nosetip shape categories for a typical ICBM trajectory as a function of nosetip material roughness.

The contributions of the Passive Nosetip Technology Program provide conceptual guidelines for developing nosetip thermal protection systems which potentially can satisfy the survival and accuracy goals of the Air Force. Reduction in the sensitivity of nosetip performance to aerodynamic and meteorological variables is the desired direction that future efforts should take. A shape-stable-nosetip (SSN) design is needed. Conceptually, an SSN would maintain a single shape in any weather situation for all trajectories and maneuvers of interest. Based on the results of the Passive Nosetip Technology Program, a passive shape-stable-nosetip design might have the following characteristics:

- The nosetip material should be sufficiently rough to promote transition at approximately 50,000 ft.
- The central core portion of the nosetip should ablate somewhat faster than the outer material so that slender, asymmetric, irregular shapes could not form.
- Both core and outer materials should be optimized to perform adequately in clear air and survive significant weather encounters.

Although incorporating a faster ablator on the nosetip central core seems contrary to improving overall nosetip performance, the analytical and experimental efforts under this program have shown that the concept is technically sound. Detailed development, test and evaluation of the concept are needed. In addition, continued assessments of the relevant aerodynamic, aerothermal, and weather phenomena will be required to support future, more severe reentry requirements.

## REFERENCES

1. Passive Nosetip Technology (PANT) Program, Interim Report Series, Volumes I through XXIII, Aerotherm Division/Acurex Corporation, January 1974 through June 1975.